Integral-direct Hartree-Fock and Møller-Plesset Perturbation Theory for Periodic Systems with Density Fitting: Application to the Benzene Crystal

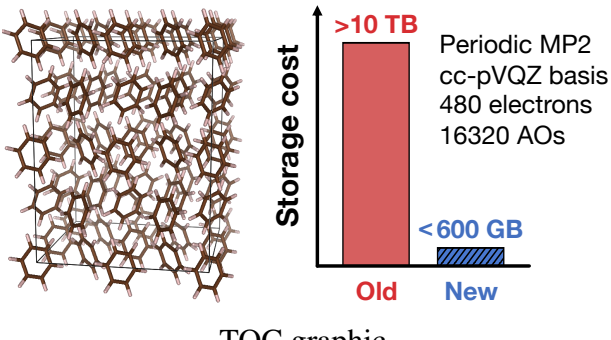
Sylvia J. Bintrim,[†] Timothy C. Berkelbach,*,[†] and Hong-Zhou Ye*,[†]

†Department of Chemistry, Columbia University, New York, New York 10027, USA ‡Center for Computational Quantum Physics, Flatiron Institute, New York, New York 10010, USA

E-mail: tim.berkelbach@gmail.com; hzyechem@gmail.com

Abstract

We present an algorithm and implementation of integral-direct, density-fitted Hartree-Fock (HF) and second-order Møller-Plesset perturbation theory (MP2) for periodic systems. The new code eliminates the formerly prohibitive storage requirements and allows us to study systems one order of magnitude larger than before at the periodic MP2 level. We demonstrate the significance of the development by studying the benzene crystal in both the thermodynamic limit and the complete basis set limit, for which we predict an MP2 cohesive energy of -72.8 kJ/mol, which is about 10--15 kJ/mol larger in magnitude than all previously reported MP2 calculations. Compared to the best theoretical estimate from literature, several modified MP2 models approach chemical accuracy in the predicted cohesive energy of the benzene crystal and hence may be promising cost-effective choices for future applications on molecular crystals.



TOC graphic

1 Introduction

Recent years have witnessed a rapid growth of interest in leveraging systematically improvable wavefunction-based quantum chemistry methods to study challenging problems in materials science. ^{1–19} These simulations, often performed using periodic boundary conditions, are computationally expensive because of the large simulation cells or dense *k*-point meshes needed to reach the thermodynamic limit ^{10,16,19,20} (TDL) and the large one-particle basis sets needed to reach the complete basis set (CBS) limit. ^{1,21–26} As in molecular calculations, the evaluation and storage of the electron-repulsion integrals (ERIs) represent a major computational bottleneck ^{27–30} in Hartree-Fock ³¹ (HF) and low-order perturbation (e.g., the second-order Møller-Plesset perturbation theory, ³² MP2) calculations, including simulations using Kohn-Sham density functional theory ^{33,34} (KS-DFT) with hybrid ^{35–37} and double-hybrid ^{38–41} exchange-correlation functionals. In Ref. 42, the commonly used density fitting (DF) technique ^{43–45} was adapted for periodic systems to reduce the computational cost of handling the periodic ERIs. The resulting implementation in the PySCF software package ^{46,47} has been used in many applications. ^{12,15,18,48,49}

This previous implementation of periodic DF⁴² is integral-indirect, meaning that the needed integrals are pre-computed and stored in memory or on disk for later use. The resources needed to store the DF integrals grow quadratically with the number of k-points and cubically with the size of the unit cell or the basis set, preventing studies of large systems in the two limits. An integral-*direct* implementation that avoids storing all DF integrals at once is thus highly desirable but is hindered by the high computational cost of evaluating these integrals.⁴² Recently, two of

us introduced a range-separated DF⁵⁰ (RSDF) algorithm for fast evaluation of the DF integrals, which, when combined with efficient integral screening,⁵¹ accelerates periodic DF by one to two orders of magnitude, as illustrated for the simulation of the benzene crystal in Fig. 1.

In this work, we leverage this significant speedup to enable an integral-direct implementation of periodic HF and MP2. The development allows us to perform periodic HF and MP2 calculations for systems one order of magnitude larger than with the previous integral-indirect implementation. We demonstrate the significance of this development by estimating the MP2 cohesive energy of the benzene crystal in both the TDL and the CBS limit. A careful comparison to existing MP2 results in the literature ^{2,4,52} suggests that they may have large finite-size and/or basis set incompleteness errors, emphasizing the challenge and importance of reaching both the TDL and the CBS limit in correlated wavefunction-based simulations of materials. We also show that various modified MP2 models ^{53–56} exhibit nearly chemical accuracy in the computed cohesive energy of the benzene crystal and hence may be promising for future applications on molecular crystals.

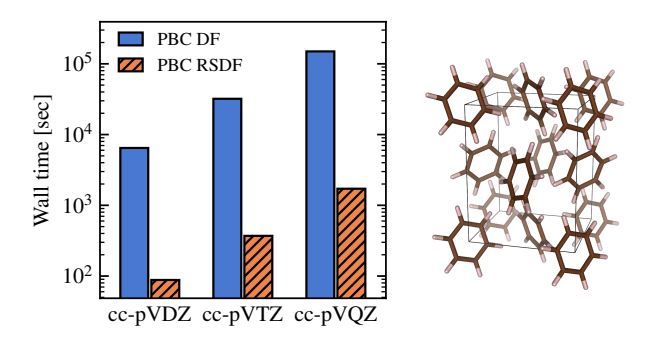


Figure 1: Wall time for calculating the DF integrals for the benzene crystal, whose unit cell is shown on the right, with Γ -point Brillouin zone sampling. The recently developed RSDF⁵⁰ (orange) algorithm accelerates the previous DF implementation (blue) by up to two orders of magnitude. All calculations are performed using PySCF on a single node with 16 CPU cores.

2 Theory

We start by briefly reviewing the formalism of periodic DF. In periodic systems, the atom-centered Gaussian-type atomic orbitals (AOs) are translational symmetry-adapted

$$\phi_{\mu}^{\mathbf{k}}(\mathbf{r}) = \sum_{\mathbf{R}} e^{i\mathbf{k}\cdot\mathbf{R}} \phi_{\mu}(\mathbf{r} - \mathbf{R})$$
 (1)

where the lattice summation runs over all unit cells in real space and k is one of the N_k crystal momenta sampled from the first Brillouin zone. The periodic DF expands the AO product density in a second, auxiliary set of translational symmetry-adapted Gaussian basis functions $\chi_P^k(r)^{42,50}$

$$\phi_{\mu}^{k_1*}(r)\phi_{\nu}^{k_2}(r) \approx \sum_{P}^{n_{\text{aux}}} d_{P\mu\nu}^{k_1k_2} \chi_P^{k_{12}}(r)$$
 (2)

so that the ERIs can be approximated as

$$V_{\mu\nu\lambda\sigma}^{k_1k_2k_3k_4} \approx \sum_{P,Q}^{n_{\text{aux}}} d_{P\mu\nu}^{k_1k_2} J_{PQ}^{k_34} d_{Q\lambda\sigma}^{k_3k_4}$$
 (3)

where $J_{PQ}^{k} = (\chi_{P}^{-k}|\chi_{Q}^{k})$ is a two-center Coulomb integral and the crystal momentum conservation requires that $k_{12} \equiv -k_1 + k_2 = -k_{34} + G$, where G is a reciprocal lattice vector. The fitting coefficients are determined by solving a linear equation

$$\sum_{Q}^{n_{\text{aux}}} J_{PQ}^{\mathbf{k}_{12}} d_{Q\mu\nu}^{\mathbf{k}_{1}\mathbf{k}_{2}} = V_{P\mu\nu}^{\mathbf{k}_{1}\mathbf{k}_{2}} \tag{4}$$

which allows one to rewrite Eq. (3) as

$$V_{\mu\nu\lambda\sigma}^{\mathbf{k}_{1}\mathbf{k}_{2}\mathbf{k}_{3}\mathbf{k}_{4}} \approx \sum_{P,Q}^{n_{\text{aux}}} V_{P\mu\nu}^{\mathbf{k}_{1}\mathbf{k}_{2}} [(\mathbf{J}^{\mathbf{k}_{34}})^{-1}]_{PQ} V_{Q\lambda\sigma}^{\mathbf{k}_{3}\mathbf{k}_{4}} = \sum_{P} \tilde{V}_{P\mu\nu}^{\mathbf{k}_{1}\mathbf{k}_{2}} \tilde{V}_{P\lambda\sigma}^{\mathbf{k}_{3}\mathbf{k}_{4}}$$
(5)

where $V_{P\mu\nu}^{k_1k_2} = (\chi_P^{-k_{12}}|\phi_\mu^{k_1*}\phi_\nu^{k_2})$, $\tilde{\mathbf{V}}^{k_1k_2} = \mathbf{L}^{k_{12}\dagger}\mathbf{V}^{k_1k_2}$, and \mathbf{L}^k is the lower-triangular matrix from the Cholesky decomposition of $(\mathbf{J}^k)^{-1}$, i.e., $(\mathbf{J}^k)^{-1} = \mathbf{L}^k\mathbf{L}^{k\dagger}$. To summarize, periodic DF factorizes the

periodic four-center ERIs into periodic two-center and three-center Coulomb integrals, and this compression is responsible for the reduced storage requirements.

However, even with DF, storage is still the main computational bottleneck for large systems: storing the three-center Coulomb integrals $V_{P\mu\nu}^{k_1k_2}$ requires $O(N_k^2n_{\rm aux}n_{\rm AO}^2)$ memory or disk space, i.e., it scales quadratically with the number of k-points and cubically with the size of the unit cell or the basis set. The basic idea of an integral-direct implementation is to calculate the three-center integrals on-the-fly to avoid the high cost of storing them all at once. In this work, using periodic integral evaluation with RSDF, we calculate the integrals in blocks and batch one of the two AO indices, which we denote by $V_{P[\mu]\nu}^{k_1k_2}$. The alternative choices to batch over the auxiliary function index or the k-points are considered in the Supporting Information, where we argue that batching over an AO index (as we do here) is best for calculations with large unit cells and small k-point meshes, but batching over k-points will be best for calculations with small unit cells and large k-point meshes (larger than $N_k \approx 5^3$ with a high-quality basis set).

We first discuss our integral-direct implementation of periodic HF, which resembles the algorithms previously developed for molecular HF calculations 57,58 but is made compatible here with the k-point symmetry that is unique to periodic systems. (See also Refs. 59–61 for recent related developments in periodic exchange evaluation.) Our goal is to calculate the Coulomb and the exchange matrices, referred to as the J-build and K-build, in an integral-direct manner. The discussion below assumes a spin-restricted mean-field state with crystalline orbitals (COs)

$$\psi_p^{\mathbf{k}}(\mathbf{r}) = \sum_{\mu}^{n_{\text{AO}}} C_{\mu p}^{\mathbf{k}} \phi_{\mu}^{\mathbf{k}}(\mathbf{r})$$
 (6)

and the corresponding CO energies ε_p^k . (The common notation of i, j, \cdots labelling n_{occ} occupied COs, a, b, \cdots labelling n_{vir} virtual COs, and p, q, \cdots labelling unspecified COs, will be used throughout the paper.) The extension to a general state that breaks spin symmetry is straightforward.

With DF, the Coulomb matrix is calculated as

$$J_{\mu\nu}^{k} = \sum_{P}^{n_{\text{aux}}} V_{P\mu\nu}^{kk} \tilde{v}_{P} \tag{7}$$

where $\tilde{\boldsymbol{v}} = (\mathbf{J}^0)^{-1} \boldsymbol{v}$,

$$v_P = \frac{1}{N_k} \sum_{k}^{N_k} \sum_{\lambda \sigma}^{n_{AO}} V_{P\lambda\sigma}^{kk} D_{\sigma\lambda}^k, \tag{8}$$

and $D_{\sigma\lambda}^{k}$ is the HF density matrix. The intermediates v and \tilde{v} are of size $O(n_{\text{aux}})$ and can always be held in memory. We note that only three-center integrals that are diagonal in k are needed, but the cubic scaling with the unit cell size or the basis set size is unchanged and can still be the bottleneck for large unit cells and/or large basis sets. To that end, we perform the tensor contractions in Eqs. (7) and (8) in blocks by batching one of the AO indices,

$$J_{[\mu]\nu}^{k} = \sum_{P}^{n_{\text{aux}}} V_{P[\mu]\nu}^{kk} \tilde{\nu}_{P} \tag{9}$$

for Eq. (7) and

$$v_P = \sum_{[\lambda]} \left(\frac{1}{N_k} \sum_{k} \sum_{\lambda \in [\lambda]} \sum_{\sigma}^{n_{AO}} V_{P\lambda\sigma}^{kk} D_{\sigma\lambda}^k \right)$$
 (10)

for Eq. (8). The batching here introduces no extra computational cost but simply avoids storing the full $V_{P_{\mu\nu}}^{kk}$ tensors.

For the exchange matrix, we adapt the occupied orbital-based K-build algorithm^{58,62} for periodic calculations with DF,

$$K_{\mu\nu}^{\mathbf{k}_{1}} = \frac{1}{N_{k}} \sum_{\mathbf{k}_{2}}^{N_{k}} \sum_{i}^{n_{\text{occ}}} \sum_{P}^{n_{\text{aux}}} \tilde{W}_{P\mu i}^{\mathbf{k}_{1}\mathbf{k}_{2}} \tilde{W}_{P\nu i}^{\mathbf{k}_{1}\mathbf{k}_{2}*}$$
(11)

where $\tilde{\mathbf{W}}^{k_1k_2} = \mathbf{L}^{k_{12}\dagger}\mathbf{W}^{k_1k_2}$ and

$$W_{P[\mu]i}^{k_1 k_2} = \sum_{\sigma}^{n_{AO}} V_{P[\mu]\sigma}^{k_1 k_2} C_{\sigma i}^{k_2} \sqrt{n_i^{k_2}}$$
(12)

with n_i^k the CO occupation number (i.e., 2 for a spin-restricted state). Like for the *J*-build, we

avoid the storage of the entire $V_{P\mu\sigma}^{k_1k_2}$ tensor in the half-transformation (12) by batching over an AO index. The alternative that batches the σ index in Eq. (12) is suboptimal because it requires repeated tensor addition to accumulate the results. Because $W_{P\mu i}^{k_1k_2}$ is smaller than $V_{P\mu\nu}^{k_1k_2}$ by a factor of n_{AO}/n_{occ} , it can be stored in its entirety for significantly larger systems. When it can be stored in memory, this completes our description of a fully direct periodic K-build.

When $W_{P\mu i}^{k_1k_2}$ does not fit in memory but does fit on disk, we use a semi-direct algorithm. In this case, we store $W_{P\mu i}^{k_1k_2}$ on disk and loaded into memory in blocks by batching the i index in Eq. (11),

$$K_{\mu\nu}^{\mathbf{k}_{1}} = \sum_{[i]} \left(\frac{1}{N_{k}} \sum_{\mathbf{k}_{2}}^{N_{k}} \sum_{i \in [i]} \sum_{P}^{n_{\text{aux}}} \tilde{W}_{P\mu i}^{\mathbf{k}_{1}\mathbf{k}_{2}} \tilde{W}_{P\nu i}^{\mathbf{k}_{1}\mathbf{k}_{2}*} \right). \tag{13}$$

If necessary, Eq. (13) can be used in a fully direct manner (i.e., using only memory), but this increases the computational cost compared to the semi-direct algorithm because each batch of the half-transformed integrals, $W_{P\mu[i]}^{k_1k_2}$, requires evaluating the entire set of three-center integrals $V_{P\mu\nu}^{k_1k_2}$. Whether the semi-direct approach is more efficient than the fully direct alternative depends on the relative cost of integral evaluation compared to writing to and reading from disk. For the current RSDF implementation, we found by numerical tests that the integral evaluation is still the computational bottleneck, and thus we use the semi-direct approach throughout this work for the K-build. We note that the situation may change depending on the compute architecture, available resources, or with further development of periodic integral evaluation (see e.g., ref 63).

Lastly, we discuss the integral-direct implementation of periodic MP2. The correlation energy for periodic MP2 is

$$E^{\text{MP2,c}} = -\frac{1}{N_k^3} \sum_{\mathbf{k_1 k_2 k_3}}^{N_k} \sum_{abij} \frac{V_{aibj}^{\mathbf{k_1 k_2 k_3 k_4 *}} (2V_{aibj}^{\mathbf{k_1 k_2 k_3 k_4}} - V_{biaj}^{\mathbf{k_3 k_2 k_1 k_4}})}{\varepsilon_a^{\mathbf{k_1}} - \varepsilon_i^{\mathbf{k_2}} + \varepsilon_b^{\mathbf{k_3}} - \varepsilon_j^{\mathbf{k_4}}}$$
(14)

where $k_4 = k_1 - k_2 + k_3 + G$ by crystal momentum conservation. With DF, the transformed ERIs

are approximated by three-index tensors

$$V_{aibj}^{\mathbf{k}_1 \mathbf{k}_2 \mathbf{k}_3 \mathbf{k}_4} \approx \sum_{P}^{n_{\text{aux}}} \tilde{U}_{Pai}^{\mathbf{k}_1 \mathbf{k}_2} \tilde{U}_{Pbj}^{\mathbf{k}_3 \mathbf{k}_4}$$

$$\tag{15}$$

where $\tilde{\mathbf{U}}^{\mathbf{k}_1\mathbf{k}_2} = \mathbf{L}^{\mathbf{k}_{12}\dagger}\mathbf{U}^{\mathbf{k}_1\mathbf{k}_2}$ and

$$U_{Pai}^{\mathbf{k}_{1}\mathbf{k}_{2}} = \sum_{\mu}^{n_{AO}} \left(\sum_{\nu}^{n_{AO}} V_{P\mu\nu}^{\mathbf{k}_{1}\mathbf{k}_{2}} C_{\nu i}^{\mathbf{k}_{2}} \right) C_{\mu a}^{\mathbf{k}_{1}*} = \sum_{\mu}^{n_{AO}} W_{P\mu i}^{\mathbf{k}_{1}\mathbf{k}_{2}} C_{\mu a}^{\mathbf{k}_{1}*}$$
(16)

are transformed three-center integrals, where we used Eq. (12) ($n_i^k = 1$ here) for the second equality. The half-transformed integrals $W_{P\mu i}^{k_1k_2}$ in Eq. (16) can be computed as discussed above for the K-build and stored on disk. These integrals are then loaded into memory in blocks by batching the i index for the second transform in Eq. (16); the alternative that batches the μ index is suboptimal due to the repeated tensor addition for accumulating the results. The $U_{Pai}^{k_1k_2}$ tensors are marginally smaller than $W_{P\mu i}^{k_1k_2}$ (by a factor of n_{AO}/n_{Vir}), and therefore have similar storage requirements. If $U_{Pai}^{k_1k_2}$ exceeds the available disk space, we compute it in blocks by batching the i index, $U_{Pai}^{k_1k_2}$, and compute the MP2 energy in blocks accordingly

$$E^{\text{MP2,c}} = \sum_{[i]} \sum_{[i]} \left(-\frac{1}{N_k^3} \sum_{k_1 k_2 k_3}^{N_k} \sum_{i \in [i]} \sum_{j \in [i]} \sum_{ab}^{n_{\text{vir}}} \cdots \right)$$
(17)

where the summand is the same as that in Eq. (14) and omitted here. Although not explored in this work, the MP2 one-particle reduced density matrix, which is useful in various reduced-scaling correlated methods based on MP2 natural orbitals, ^{21,64–69} can be evaluated in essentially the same manner. Additional approximations such as the Laplace transform that have been shown to further reduce the computational cost of canonical periodic MP2 calculations ⁹ will be explored in future work.

3 Computational details

The integral-direct algorithms presented above for periodic HF and MP2 calculations with DF are implemented in the PySCF software package ^{46,47} which uses libcint ⁷⁰ for calculating atomic integrals. We demonstrate the impact of our integral-direct algorithms by estimating the MP2 cohesive energy of the benzene crystal in both the TDL and the CBS limit. The cohesive energy of the benzene crystal has been well-studied in the literature using molecular codes via the truncated many-body expansion (MBE)^{71–74} with several correlated wavefunction methods ^{7,75} including MP2. ⁵² Two different periodic MP2 calculations have also been reported, ^{2,4} showing good agreement with each other but differing from MBE results ⁵² by about 7 kJ/mol. Here, we leverage the power of our integral-direct implementations to investigate these discrepancies through our own careful investigation of finite-size and basis set errors, ultimately finding an MP2 cohesive energy that is larger in magnitude than any of these previous studies.

All calculations reported below were performed using PySCF on a single compute node with 384 GB of memory and 1 TB of disk space. The Brillouin zone is sampled by uniform k-point meshes including the Γ -point. Finite-size errors associated with the divergence of the HF exchange integral at G = 0 are handled using a Madelung constant correction. ^{76–78} With this treatment, both the HF energy and the MP2 correlation energy exhibit a $1/N_k$ asymptotic convergence to the TDL (i.e., $N_k = \infty$) and can hence be extrapolated using the following two-point formula

$$E(\infty) = \frac{N_{k,2}^{-1}E(N_{k,1}) - N_{k,1}^{-1}E(N_{k,2})}{N_{k,2}^{-1} - N_{k,1}^{-1}}$$
(18)

for sufficiently large $N_{k,1}$ and $N_{k,2}$. We denote an extrapolation based on Eq. (18) $(N_{k,1}, N_{k,2})$.

4 Results and discussion

We first calculate the cohesive energy of the benzene crystal for the 138 K lattice geometry⁷⁹ [code BENZEN01 in the Cambridge Structure Database⁸⁰ (CSD)] using the all-electron cc-pVXZ

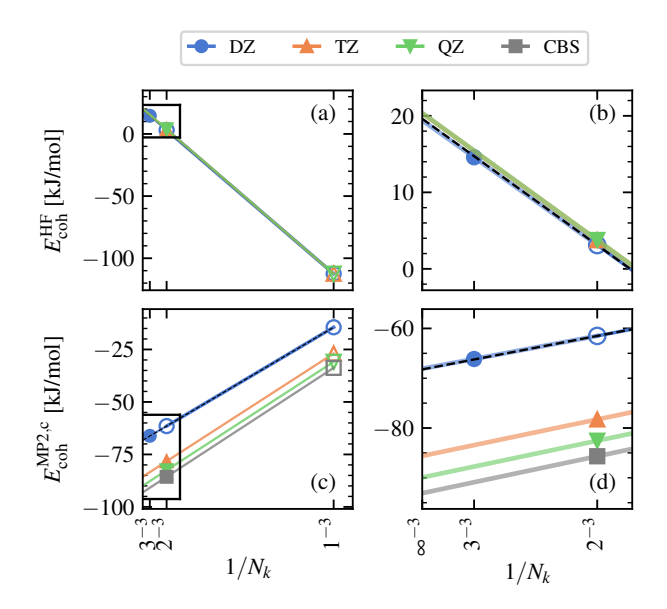


Figure 2: Thermodynamic limit convergence of the HF cohesive energy (a) and the MP2 correlation energy contribution to the cohesive energy (c) of the benzene crystal (CSD code BENZEN01) using different basis sets. Panels (b) and (d) provide zoom-in views of the corresponding region in (a) and (c) indicated by black rectangles. Hollow symbols correspond to calculations that can be performed using the previous integral-indirect implementation, while filled symbols are calculations made possible by the integral-direct implementation developed in this work. For each basis set, the TDL extrapolation based on the two largest calculations [(2³, 3³) for DZ and (1³, 2³) for others] is shown as a solid line of the corresponding color. For DZ, the (1³, 2³) TDL extrapolation is also shown as a black dashed line.

(henceforth referred to as XZ) basis sets ⁸¹ up to QZ. As shown in Fig. 1, each unit cell contains four benzene molecules, 168 electrons, and 456, 1056, and 2040 AOs with the DZ, TZ, and QZ basis sets, respectively. The corresponding cc-pVXZ-JKFIT basis sets ⁵⁸ are used for DF. The 1s core electrons of carbon are kept frozen in the MP2 calculations. The same lattice geometry and similar basis sets were used in previous MBE calculations. ^{7,52,75} The k-point convergence of the cohesive energy from our periodic HF and MP2 calculations is shown in Fig. 2 for different basis sets. For MP2, an estimate of the CBS limit of a given k-point mesh is obtained by a $1/X^3$ extrapolation using the TZ (X = 3) and the QZ (X = 4) results of the same k-point mesh. For HF, the change of the cohesive energy from TZ to QZ is less than 0.03 kJ/mol for all k-point meshes. Thus, the QZ HF results are taken as the CBS limit without further extrapolation.

With the previous integral-indirect code, we can compute the cohesive energies using $N_k = 1^3$

and 2^3 with the DZ basis set, but only using $N_k = 1^3$ with the TZ and QZ basis sets, all of which are marked by hollow symbols in Fig. 2. Therefore, the TDL extrapolation using Eq. (18) can only be performed with DZ (black dashed lines) and gives a cohesive energy of 19.6 kJ/mol for HF and -48.6 kJ/mol for MP2, respectively. The quality of this $(1^3, 2^3)$ TDL extrapolation is, however, questionable due to the use of relatively small k-point meshes. In addition, the MP2 cohesive energy at Γ -point obtained using the DZ basis set is about 20 kJ/mol higher than the estimated CBS limit as shown in Fig. 2(c), indicating a large basis set incompleteness error. A simple composite estimate, based on these minimal data points, suggests an MP2 cohesive energy of -67.9 kJ/mol in the combined TDL and CBS limit, which underestimates our best estimate by about 5 kJ/mol (*vide infra*).

The integral-direct code developed in this work allows us to obtain the cohesive energies for k-point meshes one order of magnitude larger than before, i.e., $N_k = 3^3$ with DZ and $N_k = 2^3$ with TZ and QZ, as marked by filled symbols in Fig. 2. For DZ, a $(2^3, 3^3)$ TDL extrapolation using Eq. (18) (blue solid lines) gives a cohesive energy of 19.4 kJ/mol for HF and -48.7 kJ/mol for MP2, respectively, which agree very well with the $(1^3, 2^3)$ TDL extrapolation discussed above [see also the overlay of the blue solid line and the black dashed line in Fig. 2(b,d)]. The nearly quantitative agreement justifies a $(1^3, 2^3)$ TDL extrapolation for larger basis sets followed by a composite correction from the difference between the $(2^3, 3^3)$ and $(1^3, 2^3)$ TDL extrapolations of DZ (which we denote by Δ DZ). The obtained cohesive energies in the TDL for various basis sets and the estimated CBS limit are listed in Table 1, along with results from the literature for comparison.

The cohesive energy from our periodic HF calculations in the CBS limit (20.2 kJ/mol) agrees quantitatively with that obtained from a MBE truncated to tetramers. Our estimated MP2 cohesive energy in the CBS limit (-72.8 kJ/mol) is about 9 kJ/mol larger in magnitude than the MBE result in ref 52, which considered only dimer interactions. We attribute the difference to the neglect of contributions from trimers and tetramers, which have been shown to cause a sizable error for the benzene crystal.

Table 1: Cohesive energy of the benzene crystal. Results are reported for the 138 K lattice structure ⁷⁹ (CSD code BENZEN01) unless otherwise specified.

	Basis set	TDL	$E_{\rm coh}$ [kJ/mol]		
			HF	MP2	
MBE					
	cc-pV5Z		20.2	N/A	ref 7
	(T,Q)-CBS		N/A	-64.0	ref 52
Periodic					
	cc-pVDZ	$(2^3, 3^3)$	19.4	-48.7	this work
	cc-pVTZ	$(1^3, 2^3) + \Delta DZ$	20.1	-65.5	this work
	cc-pVQZ	$(1^3, 2^3) + \Delta DZ$	20.2	-69.8	this work
	(T,Q)-CBS	$(1^3, 2^3) + \Delta DZ$	20.2	-72.8	this work
	p-aug-6-31G**a	N/A	N/A	-56.6 ^b	ref 2 ^c
	p-aug-6-31G**a	$(1^3, 2^3)$	20.0	-67.9	this work ^c
	cc-TZVP ^d	$2 \times 1 \times 2^{e}$	21.2	-58.7	ref 4 ^c
	cc-TZVP ^d	$(1^3, 2^3)$	20.5	-69.5	this work ^c

^a The diffuse p function for H and d function for C from the aug-cc-pVDZ basis set are added 6-31G**.

Also listed in Table 1 are the cohesive energies from two periodic MP2 studies in literature ^{2,4} for the 123 K lattice structure ⁸³ (CSD code BENZEN07). Ref 2 uses a partially augmented 6-31G** (p-aug-6-31G**) basis set and obtains an MP2 cohesive energy of –56.6 kJ/mol, while ref 4 uses a TZ-quality basis set (cc-TZVP) and Goedecker-Teter-Hutter (GTH) pseudopotentials ^{86,87} and predicts a similar value of –58.7 kJ/mol. Despite the reasonable agreement between them, these values are noticeably smaller in magnitude, by up to 16 kJ/mol, than our best estimate in the TDL and the CBS limit. We repeated our MP2 calculations using the same basis sets and lattice structure as in these previous works, but extrapolated to the TDL based on the (1³, 2³) scheme established above. As shown in Table 1, the difference between our MP2 cohesive energies and the literature values suggests that the latter have a finite-size error of about 11 kJ/mol. The difference from our best estimate in the CBS limit reveals a basis set incompleteness error of about 3 and

^b Using local MP2⁸² (LMP2).

^c Using the 123 K lattice structure ⁸³ (CSD code BENZEN07).

^d Using the GTH pseudopotential optimized for HF. ⁸⁴

^e Using the truncated Coulomb potential ⁸⁵ for HF.

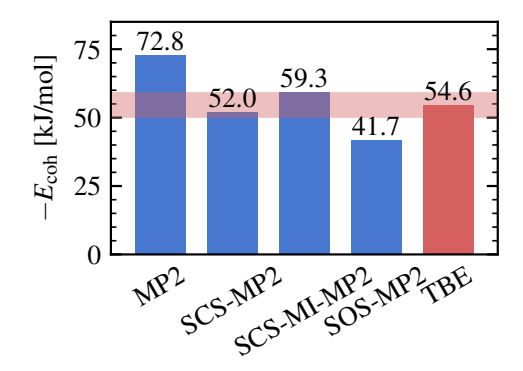


Figure 3: Cohesive energy of the benzene crystal (138 K lattice structure) computed from MP2 and its empirical modifications in both the TDL $[(1^3, 2^3) + \Delta DZ]$ and the CBS limit [(T,Q)]. The theoretical best estimate (TBE) from ref 7 is plotted for comparison. The red shaded area indicates ± 1 kcal/mol from the TBE.

5 kJ/mol for the cc-TZVP and the p-aug-6-31G** basis sets, respectively (we have numerically confirmed that the two crystal structures have cohesive energies that differ by less than 1 kJ/mol). These comparisons demonstrate the challenge of reaching the combined TDL and CBS limit and the value of our integral-direct algorithms that enable calculations with large *k*-point meshes and large basis sets.

Finally, we gauge the performance of various empirically modified MP2 models that are commonly used for molecules, ^{53–56} and which we have found, in forthcoming work from our group, ⁸⁸ to significantly improve the cohesive properties of covalently bound semiconductors and insulators. These models are based on scaling the correlation energy of different spin components [i.e., same-spin (SS) and opposite-spin (OS)] with different coefficients

$$E_{\text{modified}}^{\text{MP2,c}}(c_{\text{SS}}, c_{\text{OS}}) = c_{\text{SS}} E_{\text{SS}}^{\text{MP2,c}} + c_{\text{OS}} E_{\text{OS}}^{\text{MP2,c}}$$
(19)

where the unmodified MP2 model is recovered for $c_{\rm SS} = c_{\rm OS} = 1$. Figure 3 shows the benzene crystal cohesive energy computed from three such models in the TDL and the CBS limit, along with the theoretical best estimate (TBE) from ref 7 for comparison. All modified MP2 models correct for the known overestimation of the dispersion interaction by unmodified MP2. ^{89,90} The general-purpose spin-component-scaled (SCS) model ⁵³ and the SCS-molecular interaction (SCS-

MI) model⁵⁵ parameterized for reproducing the CCSD(T)⁹¹ intermolecular interactions both give results within chemical accuracy (1 kcal/mol or 4.2 kJ/mol; see the red shaded area in Fig. 3), while the scaled-opposite-spin (SOS) model⁵⁴ significantly underestimates the TBE by about 13 kJ/mol, which is consistent with previous literature results.^{55,92}

5 Conclusion

To conclude, in this work we reported an integral-direct implementation of periodic HF and MP2 with DF, which is made possible by our recent developments in periodic DF integral evaluation. ^{50,51} The development enables us to study systems one order of magnitude larger than before and allowed us to estimate the MP2 cohesive energy of the benzene crystal in both the TDL and the CBS limit, which in turn corrects the previously reported MP2 results from the literature. Several modified MP2 models were shown to exhibit nearly chemical accuracy for the benzene crystal cohesive energy, which suggests that modified MP2 models and the closely related double-hybrid KS-DFT ^{17,38–41,93} may be cost-effective choices for crystal structure prediction.

The integral-direct code developed in this work has essentially eliminated the storage bottlenecks of large, periodic electronic structure calculations at the presented levels of theory. However,
it does not lower their computational scaling, which is now the bottleneck that precludes larger calculations. For truly large-scale applications, local approximations in one form or another 62,94–98 are
necessary, and we expect that the work presented here will be essential in the benchmarking and
development of those methods.

Acknowledgements

We thank Dr. Xiao Wang for helpful discussions. This work was supported by the National Science Foundation under Grant No. DGE-1644869 (S.J.B.) and Grant No. OAC-1931321 (H.-Z.Y.). We acknowledge computing resources from Columbia University's Shared Research Computing Facility project, which is supported by NIH Research Facility Improvement Grant 1G20RR030893-01,

and associated funds from the New York State Empire State Development, Division of Science Technology and Innovation (NYSTAR) Contract C090171, both awarded April 15, 2010. The Flatiron Institute is a division of the Simons Foundation.

Supporting Information

See the supporting information for (i) a review of periodic DF and the RSDF algorithm and (ii) a comparison of different strategies for batching the three-center integrals.

Data availability statement

The data that support the findings of this study are available from the corresponding author upon reasonable request.

References

- (1) Marsman, M.; Grüneis, A.; Paier, J.; Kresse, G. Second-order Møller-Plesset perturbation theory applied to extended systems. I. Within the projector-augmented-wave formalism using a plane wave basis set. *J. Chem. Phys.* **2009**, *130*, 184103.
- (2) Maschio, L.; Civalleri, B.; Ugliengo, P.; Gavezzotti, A. Intermolecular Interaction Energies in Molecular Crystals: Comparison and Agreement of Localized Møller-Plesset 2, Dispersion-Corrected Density Functional, and Classical Empirical Two-Body Calculations. *J. Phys. Chem. A* 2011, 115, 11179–11186.
- (3) Müller, C.; Paulus, B. Wavefunction-based electron correlation methods for solids. *Phys. Chem. Chem. Phys.* **2012**, *14*, 7605–7614.
- (4) Del Ben, M.; Hutter, J.; Vande Vondele, J. Second-Order Møller-Plesset Perturbation Theory

- in the Condensed Phase: An Efficient and Massively Parallel Gaussian and Plane Waves Approach. *J. Chem. Theory Comput.* **2012**, *8*, 4177–4188.
- (5) Del Ben, M.; Hutter, J.; VandeVondele, J. Electron Correlation in the Condensed Phase from a Resolution of Identity Approach Based on the Gaussian and Plane Waves Scheme. *J. Chem. Theory Comput.* **2013**, *9*, 2654–2671.
- (6) Booth, G. H.; Grüneis, A.; Kresse, G.; Alavi, A. Towards an exact description of electronic wavefunctions in real solids. *Nature* **2013**, *493*, 365–370.
- (7) Yang, J.; Hu, W.; Usvyat, D.; Matthews, D.; Schütz, M.; Chan, G. K.-L. Ab initio determination of the crystalline benzene lattice energy to sub-kilojoule/mole accuracy. *Science* **2014**, *345*, 640–643.
- (8) McClain, J.; Sun, Q.; Chan, G. K.-L.; Berkelbach, T. C. Gaussian-Based Coupled-Cluster Theory for the Ground-State and Band Structure of Solids. J. Chem. Theory Comput. 2017, 13, 1209–1218.
- (9) Schäfer, T.; Ramberger, B.; Kresse, G. Quartic scaling MP2 for solids: A highly parallelized algorithm in the plane wave basis. *J. Chem. Phys.* **2017**, *146*, 104101.
- (10) Gruber, T.; Liao, K.; Tsatsoulis, T.; Hummel, F.; Grüneis, A. Applying the Coupled-Cluster Ansatz to Solids and Surfaces in the Thermodynamic Limit. *Phys. Rev. X* **2018**, *8*, 021043.
- (11) Zhang, I. Y.; Grüneis, A. Coupled Cluster Theory in Materials Science. *Front. Mater.* **2019**, *6*, 123.
- (12) Wang, X.; Berkelbach, T. C. Excitons in Solids from Periodic Equation-of-Motion Coupled-Cluster Theory. *J. Chem. Theory Comput.* **2020**, *16*, 3095–3103.
- (13) Lau, B. T. G.; Knizia, G.; Berkelbach, T. C. Regional Embedding Enables High-Level Quantum Chemistry for Surface Science. *J. Phys. Chem. Lett.* **2021**, *12*, 1104–1109.

- (14) Lange, M. F.; Berkelbach, T. C. Improving MP2 bandgaps with low-scaling approximations to EOM-CCSD. *J. Chem. Phys.* **2021**, *155*, 081101.
- (15) Wang, X.; Berkelbach, T. C. Absorption Spectra of Solids from Periodic Equation-of-Motion Coupled-Cluster Theory. *J. Chem. Theory Comput.* **2021**, *17*, 6387–6394.
- (16) Mihm, T. N.; Schäfer, T.; Ramadugu, S. K.; Weiler, L.; Grüneis, A.; Shepherd, J. J. A shortcut to the thermodynamic limit for quantum many-body calculations of metals. *Nat. Comput. Sci.* **2021**, *1*, 801–808.
- (17) Wang, Y.; Li, Y.; Chen, J.; Zhang, I. Y.; Xu, X. Doubly Hybrid Functionals Close to Chemical Accuracy for Both Finite and Extended Systems: Implementation and Test of XYG3 and XYGJ-OS. *JACS Au* **2021**, *1*, 543–549.
- (18) Nusspickel, M.; Booth, G. H. Systematic Improvability in Quantum Embedding for Real Materials. *Phys. Rev. X* **2022**, *12*, 011046.
- (19) Neufeld, V. A.; Ye, H.-Z.; Berkelbach, T. C. Ground-state properties of metallic solids from ab initio coupled-cluster theory. 2022.
- (20) Grüneis, A.; Marsman, M.; Kresse, G. Second-order Møller-Plesset perturbation theory applied to extended systems. II. Structural and energetic properties. *J. Chem. Phys.* **2010**, *133*, 074107.
- (21) Grüneis, A.; Booth, G. H.; Marsman, M.; Spencer, J.; Alavi, A.; Kresse, G. Natural Orbitals for Wave Function Based Correlated Calculations Using a Plane Wave Basis Set. *J. Chem. Theory Comput.* **2011**, *7*, 2780–2785.
- (22) Shepherd, J. J.; Grüneis, A.; Booth, G. H.; Kresse, G.; Alavi, A. Convergence of many-body wave-function expansions using a plane-wave basis: From homogeneous electron gas to solid state systems. *Phys. Rev. B* **2012**, *86*, 035111.

- (23) Booth, G. H.; Tsatsoulis, T.; Chan, G. K.-L.; Grüneis, A. From plane waves to local Gaussians for the simulation of correlated periodic systems. *J. Chem. Phys.* **2016**, *145*, 084111.
- (24) Callahan, J. M.; Lange, M. F.; Berkelbach, T. C. Dynamical correlation energy of metals in large basis sets from downfolding and composite approaches. *J. Chem. Phys.* **2021**, *154*, 211105.
- (25) Lee, J.; Feng, X.; Cunha, L. A.; Gonthier, J. F.; Epifanovsky, E.; Head-Gordon, M. Approaching the basis set limit in Gaussian-orbital-based periodic calculations with transferability: Performance of pure density functionals for simple semiconductors. *J. Chem. Phys.* 2021, 155, 164102.
- (26) Ye, H.-Z.; Berkelbach, T. C. Correlation-Consistent Gaussian Basis Sets for Solids Made Simple. *J. Chem. Theory Comput.* **2022**, *18*, 1595–1606.
- (27) Schwegler, E.; Challacombe, M. Linear scaling computation of the Hartree-Fock exchange matrix. *J. Chem. Phys.* **1996**, *105*, 2726–2734.
- (28) Challacombe, M.; Schwegler, E. Linear scaling computation of the Fock matrix. *J. Chem. Phys.* **1997**, *106*, 5526–5536.
- (29) Ochsenfeld, C.; White, C. A.; Head-Gordon, M. Linear and sublinear scaling formation of Hartree-Fock-type exchange matrices. *J. Chem. Phys.* **1998**, *109*, 1663–1669.
- (30) Shao, Y.; Head-Gordon, M. An improved *J* matrix engine for density functional theory calculations. *Chem. Phys. Lett.* **2000**, *323*, 425–433.
- (31) Roothaan, C. C. J. New Developments in Molecular Orbital Theory. *Rev. Mod. Phys.* **1951**, 23, 69–89.
- (32) Møller, C.; Plesset, M. S. Note on an Approximation Treatment for Many-Electron Systems. *Phys. Rev.* **1934**, *46*, 618–622.

- (33) Hohenberg, P.; Kohn, W. Inhomogeneous Electron Gas. Phys. Rev. 1964, 136, B864–B871.
- (34) Kohn, W.; Sham, L. J. Self-Consistent Equations Including Exchange and Correlation Effects. *Phys. Rev.* **1965**, *140*, A1133–A1138.
- (35) Becke, A. D. Density-functional thermochemistry. III. The role of exact exchange. *J. Chem. Phys.* **1993**, *98*, 5648–5652.
- (36) Adamo, C.; Barone, V. Toward reliable density functional methods without adjustable parameters: The PBE0 model. *J. Chem. Phys.* **1999**, *110*, 6158–6170.
- (37) Heyd, J.; Scuseria, G. E.; Ernzerhof, M. Hybrid functionals based on a screened Coulomb potential. *J. Chem. Phys.* **2003**, *118*, 8207–8215.
- (38) Grimme, S. Semiempirical hybrid density functional with perturbative second-order correlation. *J. Chem. Phys.* **2006**, *124*, 034108.
- (39) Zhang, Y.; Xu, X.; Goddard, W. A. Doubly hybrid density functional for accurate descriptions of nonbond interactions, thermochemistry, and thermochemical kinetics. *Proc. Natl. Acad. Sci.* **2009**, *106*, 4963–4968.
- (40) Kozuch, S.; Gruzman, D.; Martin, J. M. L. DSD-BLYP: A General Purpose Double Hybrid Density Functional Including Spin Component Scaling and Dispersion Correction. J. Phys. Chem. C 2010, 114, 20801–20808.
- (41) Kozuch, S.; Martin, J. M. L. DSD-PBEP86: in search of the best double-hybrid DFT with spin-component scaled MP2 and dispersion corrections. *Phys. Chem. Chem. Phys.* **2011**, *13*, 20104–20107.
- (42) Sun, Q.; Berkelbach, T. C.; McClain, J. D.; Chan, G. K.-L. Gaussian and plane-wave mixed density fitting for periodic systems. *J. Chem. Phys.* **2017**, *147*, 164119.
- (43) Whitten, J. L. Coulombic potential energy integrals and approximations. *J. Chem. Phys.* **1973**, 58, 4496–4501.

- (44) Dunlap, B. I.; Connolly, J. W. D.; Sabin, J. R. On some approximations in applications of $X\alpha$ theory. *J. Chem. Phys.* **1979**, *71*, 3396–3402.
- (45) Mintmire, J. W.; Dunlap, B. I. Fitting the Coulomb potential variationally in linear-combination-of-atomic-orbitals density-functional calculations. *Phys. Rev. A* **1982**, 25, 88–95.
- (46) Sun, Q.; Berkelbach, T. C.; Blunt, N. S.; Booth, G. H.; Guo, S.; Li, Z.; Liu, J.; McClain, J. D.; Sayfutyarova, E. R.; Sharma, S.; Wouters, S.; Chan, G. K.-L. PySCF: the Python-based simulations of chemistry framework. *Wiley Interdiscip. Rev. Comput. Mol. Sci* **2018**, 8, e1340.
- (47) Sun, Q.; Zhang, X.; Banerjee, S.; Bao, P.; Barbry, M.; Blunt, N. S.; Bogdanov, N. A.; Booth, G. H.; Chen, J.; Cui, Z.-H.; Eriksen, J. J.; Gao, Y.; Guo, S.; Hermann, J.; Hermes, M. R.; Koh, K.; Koval, P.; Lehtola, S.; Li, Z.; Liu, J.; Mardirossian, N.; McClain, J. D.; Motta, M.; Mussard, B.; Pham, H. Q.; Pulkin, A.; Purwanto, W.; Robinson, P. J.; Ronca, E.; Sayfutyarova, E. R.; Scheurer, M.; Schurkus, H. F.; Smith, J. E. T.; Sun, C.; Sun, S.-N.; Upadhyay, S.; Wagner, L. K.; Wang, X.; White, A.; Whitfield, J. D.; Williamson, M. J.; Wouters, S.; Yang, J.; Yu, J. M.; Zhu, T.; Berkelbach, T. C.; Sharma, S.; Sokolov, A. Y.; Chan, G. K.-L. Recent developments in the PySCF program package. *J. Chem. Phys.* 2020, 153, 024109.
- (48) Zhu, T.; Chan, G. K.-L. All-Electron Gaussian-Based *G0W0* for Valence and Core Excitation Energies of Periodic Systems. *J. Chem. Theory Comput.* **2021**, *17*, 727–741.
- (49) Zhu, T.; Chan, G. K.-L. Ab Initio Full Cell *GW* + DMFT for Correlated Materials. *Phys. Rev. X* **2021**, *11*, 021006.
- (50) Ye, H.-Z.; Berkelbach, T. C. Fast periodic Gaussian density fitting by range separation. *J. Chem. Phys.* **2021**, *154*, 131104.
- (51) Ye, H.-Z.; Berkelbach, T. C. Tight distance-dependent estimators for screening two-center

- and three-center short-range Coulomb integrals over Gaussian basis functions. *J. Chem. Phys.* **2021**, *155*, 124106.
- (52) Ringer, A.; Sherrill, C. First Principles Computation of Lattice Energies of Organic Solids: The Benzene Crystal. *Eur. J. Chem.* **2008**, *14*, 2542–2547.
- (53) Grimme, S. Improved second-order Møller-Plesset perturbation theory by separate scaling of parallel- and antiparallel-spin pair correlation energies. *J. Chem. Phys.* **2003**, *118*, 9095–9102.
- (54) Jung, Y.; Lochan, R. C.; Dutoi, A. D.; Head-Gordon, M. Scaled opposite-spin second order M
 øller-Plesset correlation energy: An economical electronic structure method. *J. Chem. Phys.* 2004, 121, 9793–9802.
- (55) JR., R. A. D.; Head-Gordon, M. Optimized spin-component scaled second-order Møller-Plesset perturbation theory for intermolecular interaction energies. *Mol. Phys.* 2007, 105, 1073–1083.
- (56) Tan, S.; Barrera Acevedo, S.; Izgorodina, E. I. Generalized spin-ratio scaled MP2 method for accurate prediction of intermolecular interactions for neutral and ionic species. *J. Chem. Phys.* **2017**, *146*, 064108.
- (57) Neese, F.; Olbrich, G. Efficient use of the resolution of the identity approximation in time-dependent density functional calculations with hybrid density functionals. *Chem. Phys. Lett.* **2002**, *362*, 170–178.
- (58) Weigend, F. A fully direct RI-HF algorithm: Implementation, optimised auxiliary basis sets, demonstration of accuracy and efficiency. *Phys. Chem. Chem. Phys.* **2002**, *4*, 4285–4291.
- (59) Sun, Q. Exact exchange matrix of periodic Hartree-Fock theory for all-electron simulations. 2021.

- (60) Sharma, S.; White, A. F.; Beylkin, G. Fast exchange with Gaussian basis set using robust pseudospectral method. 2022.
- (61) Lee, J.; Rettig, A.; Feng, X.; Epifanovsky, E.; Head-Gordon, M. Faster Exact Exchange for Solids via occ-RI-K: Application to Combinatorially Optimized Range-Separated Hybrid Functionals for Simple Solids Near the Basis Set Limit. 2022.
- (62) Köppl, C.; Werner, H.-J. Parallel and Low-Order Scaling Implementation of Hartree-Fock Exchange Using Local Density Fitting. *J. Chem. Theory Comput.* **2016**, *12*, 3122–3134.
- (63) Sharma, S.; Beylkin, G. Efficient Evaluation of Two-Center Gaussian Integrals in Periodic Systems. *J. Chem. Theory Comput.* **2021**, *17*, 3916–3922.
- (64) Jensen, H. J. A.; Jørgensen, P.; Ågren, H.; Olsen, J. Second-order Møller-Plesset perturbation theory as a configuration and orbital generator in multiconfiguration self-consistent field calculations. *J. Chem. Phys.* **1988**, 88, 3834–3839.
- (65) Landau, A.; Khistyaev, K.; Dolgikh, S.; Krylov, A. I. Frozen natural orbitals for ionized states within equation-of-motion coupled-cluster formalism. *J. Chem. Phys.* **2010**, *132*, 014109.
- (66) Kumar, A.; Crawford, T. D. Frozen Virtual Natural Orbitals for Coupled-Cluster Linear-Response Theory. *J. Phys. Chem. A* **2017**, *121*, 708–716.
- (67) Guo, Y.; Becker, U.; Neese, F. Comparison and combination of "direct" and fragment based local correlation methods: Cluster in molecules and domain based local pair natural orbital perturbation and coupled cluster theories. *J. Chem. Phys.* **2018**, *148*, 124117.
- (68) Nagy, P. R.; Kállay, M. Approaching the Basis Set Limit of CCSD(T) Energies for Large Molecules with Local Natural Orbital Coupled-Cluster Methods. J. Chem. Theory Comput. 2019, 15, 5275–5298.
- (69) Lange, M. F.; Berkelbach, T. C. Active space approaches combining coupled-cluster and perturbation theory for ground states and excited states. *Mol. Phys.* **2020**, *118*, e1808726.

- (70) Sun, Q. Libcint: An efficient general integral library for Gaussian basis functions. *J. Comput. Chem.* **2015**, *36*, 1664–1671.
- (71) Stoll, H. Correlation energy of diamond. *Phys. Rev. B* **1992**, *46*, 6700–6704.
- (72) Hirata, S.; Valiev, M.; Dupuis, M.; Xantheas, S. S.; Sugiki, S.; Sekino, H. Fast electron correlation methods for molecular clusters in the ground and excited states. *Mol. Phys.* **2005**, *103*, 2255–2265.
- (73) Paulus, B. The method of increments-a wavefunction-based ab initio correlation method for solids. *Phys. Rep.* **2006**, *428*, 1–52.
- (74) Kamiya, M.; Hirata, S.; Valiev, M. Fast electron correlation methods for molecular clusters without basis set superposition errors. *J. Chem. Phys.* **2008**, *128*, 074103.
- (75) Schweizer, W. B.; Dunitz, J. D. Quantum Mechanical Calculations for Benzene Dimer Energies: Present Problems and Future Challenges. *J. Chem. Theory Comput.* **2006**, 2, 288–291.
- (76) Paier, J.; Marsman, M.; Hummer, K.; Kresse, G.; Gerber, I. C.; Ángyán, J. G. Screened hybrid density functionals applied to solids. *J. Chem. Phys.* **2006**, *124*, 154709.
- (77) Broqvist, P.; Alkauskas, A.; Pasquarello, A. Hybrid-functional calculations with plane-wave basis sets: Effect of singularity correction on total energies, energy eigenvalues, and defect energy levels. *Phys. Rev. B* **2009**, *80*, 085114.
- (78) Sundararaman, R.; Arias, T. A. Regularization of the Coulomb singularity in exact exchange by Wigner-Seitz truncated interactions: Towards chemical accuracy in nontrivial systems. *Phys. Rev. B* **2013**, *87*, 165122.
- (79) Bacon, G. E.; Curry, N. A.; Wilson, S. A.; Spence, R. A crystallographic study of solid benzene by neutron diffraction. *Proc. R. Soc. A: Math. Phys. Eng. Sci.* **1964**, 279, 98–110.
- (80) Groom, C. R.; Bruno, I. J.; Lightfoot, M. P.; Ward, S. C. The Cambridge Structural Database. *Acta Crystallogr. B: Struct. Sci. Cryst. Eng. Mater.* **2016**, *72*, 171–179.

- (81) Dunning, T. H. Gaussian basis sets for use in correlated molecular calculations. I. The atoms boron through neon and hydrogen. *J. Chem. Phys.* **1989**, *90*, 1007–1023.
- (82) Pisani, C.; Busso, M.; Capecchi, G.; Casassa, S.; Dovesi, R.; Maschio, L.; Zicovich-Wilson, C.; Schütz, M. Local-MP2 electron correlation method for nonconducting crystals. J. Chem. Phys. 2005, 122, 094113.
- (83) Jeffrey, G. A.; Ruble, J. R.; McMullan, R. K.; Pople, J. A.; Cox, E. G. The crystal structure of deuterated benzene. *Proc. R. Soc. A: Math. Phys. Eng. Sci.* **1987**, *414*, 47–57.
- (84) Hutter, J. New Optimization of GTH Pseudopotentials for PBE, SCAN, PBE0 Functionals. GTH Pseudopotentials for Hartree-Fock. NLCC Pseudopotentials for PBE. https://github.com/juerghutter/GTH, 2019.
- (85) Spencer, J.; Alavi, A. Efficient calculation of the exact exchange energy in periodic systems using a truncated Coulomb potential. *Phys. Rev. B* **2008**, 77, 193110.
- (86) Goedecker, S.; Teter, M.; Hutter, J. Separable dual-space Gaussian pseudopotentials. *Phys. Rev. B* **1996**, *54*, 1703–1710.
- (87) Hartwigsen, C.; Goedecker, S.; Hutter, J. Relativistic separable dual-space Gaussian pseudopotentials from H to Rn. *Phys. Rev. B* **1998**, *58*, 3641–3662.
- (88) Goldzak, T.; Wang, X.; Ye, H.-Z.; Berkelbach, T. C. unpublished.
- (89) Cybulski, S. M.; Lytle, M. L. The origin of deficiency of the supermolecule second-order Møller-Plesset approach for evaluating interaction energies. *J. Chem. Phys.* **2007**, *127*, 141102.
- (90) Heβelmann, A. Improved supermolecular second order Møller-Plesset intermolecular interaction energies using time-dependent density functional response theory. J. Chem. Phys. 2008, 128, 144112.

- (91) Raghavachari, K.; Trucks, G. W.; Pople, J. A.; Head-Gordon, M. A fifth-order perturbation comparison of electron correlation theories. *Chem. Phys. Lett.* **1989**, *157*, 479–483.
- (92) Lochan, R. C.; Jung, Y.; Head-Gordon, M. Scaled Opposite Spin Second Order Møller-Plesset Theory with Improved Physical Description of Long-Range Dispersion Interactions. *J. Phys. Chem. A* 2005, 109, 7598–7605.
- (93) Stein, F.; Hutter, J.; Rybkin, V. V. Double-Hybrid DFT Functionals for the Condensed Phase: Gaussian and Plane Waves Implementation and Evaluation. *Molecules* **2020**, *25*.
- (94) Maschio, L.; Usvyat, D.; Manby, F. R.; Casassa, S.; Pisani, C.; Schütz, M. Fast local-MP2 method with density-fitting for crystals. I. Theory and algorithms. *Phys. Rev. B* **2007**, *76*, 075101.
- (95) Usvyat, D.; Maschio, L.; Manby, F. R.; Casassa, S.; Schütz, M.; Pisani, C. Fast local-MP2 method with density-fitting for crystals. II. Test calculations and application to the carbon dioxide crystal. *Phys. Rev. B* **2007**, *76*, 075102.
- (96) Pinski, P.; Riplinger, C.; Valeev, E. F.; Neese, F. Sparse maps-A systematic infrastructure for reduced-scaling electronic structure methods. I. An efficient and simple linear scaling local MP2 method that uses an intermediate basis of pair natural orbitals. *J. Chem. Phys.* 2015, 143, 034108.
- (97) Tew, D. P. Communication: Quasi-robust local density fitting. *J. Chem. Phys.* **2018**, *148*, 011102.
- (98) Wang, X.; Lewis, C. A.; Valeev, E. F. Efficient evaluation of exact exchange for periodic systems via concentric atomic density fitting. *J. Chem. Phys.* **2020**, *153*, 124116.